**Sustainable Marine Structures**
https://journals.nasspublishing.com/index.php/sms

ARTICLE

# Tsunami Preparedness in the Coastal Tourism Area of Palabuhanratu Bay, West Java

***Wahyu Widiyanto*** [1]***, Sanidhya Nika Purnomo*** [1] ***, Muhammad Azmy Ikhsani*** [2]***, Alena Najwa Lulu Birki Zain***[1]***, Amru Muyassar Raharjo*** [1]***, Hidayat*** [1]***, Muhammad Wisnu Zulva Al Azmi*** [1]***, Haidar Fadhila Rahman*** [3]

[1] *Department of Civil Engineering, Universitas Jenderal Soedirman, Purwokerto 53122, Indonesia*

[2] *Department of Architecture, Universitas Jenderal Soedirman, Purwokerto 53122, Indonesia*

[3] *Department of Civil and Construction Engineering, National Yunlin University of Science and Technology, Douliu City 64002, Taiwan*

## ABSTRACT

The Sunda Strait segment constitutes a subduction zone near the periphery of the Indonesian Ring of Fire that has not released its energy through a significant earthquake for an extended period, hence referred to as a seismic gap. The anticipated magnitude of this earthquake is projected to be MW 8.7. If this possibility occurs, it will lead to a significant earthquake and tsunami. Consequently, community preparedness is imperative. This article examines inexpensive and easily executable preparations. Palabuhanratu Bay, a heavily populated and geographically distinctive tourism destination in West Java, was chosen. A tsunami simulation will be executed to ascertain the height, arrival timing, and potential inundation area of the tsunami. An efficient evacuation path will be devised. A community-based mitigation strategy is presented, involving the installation of lifebuoys that serve as lifesaving devices during a tsunami, aimed at decreasing drowning fatalities caused by runup. Simulation results in the research region show a tsunami height exceeding the major tsunami category (>3 m), with the observation site recording a height of 7–10 m. The tsunami arrival time varies between 17 and 23 min. The projected area of probable inundation is 6.24 $km^2$. Dijkstra's algorithm was employed to identify 20 alternate

*CORRESPONDING AUTHOR:
Wahyu Widiyanto, Department of Civil Engineering, Faculty of Engineering, Universitas Jenderal Soedirman, Purwokerto 53122, Indonesia; Email: wahyu.widiyanto@unsoed.ac.id

ARTICLE INFO
Received: 27 October 2025 | Revised: 30 December 2025 | Accepted: 28 January 2026 | Published Online: 12 February 2026
DOI: https://doi.org/10.36956/sms.v8i1.2868

CITATION
Widiyanto, W., Purnomo, S.N., Ikhsani, M.A., et al., 2026. Tsunami Preparedness in the Coastal Tourism Area of Palabuhanratu Bay, West Java. Sustainable Marine Structures. 8(1): 115–141. DOI: https://doi.org/10.36956/sms.v8i1.2868

evacuation routes at each observation location. Evacuation durations ranged from 16 to 18 min, with distances varying from 390 m to 1040 m. Based on insights from prior tsunamis, many survivors survived by grasping floating debris; this study suggests the strategic placement of denser coastal buoys along designated evacuation pathways.

***Keywords:*** Tsunami; Mitigation; Preparedness; Evacuation; Lifebuoy; Megathrust; Sunda Strait

# 1. Introduction

Indonesia is an archipelagic nation located at the intersection of three major tectonic plates: the Indo-Australian, Eurasian, and Pacific Plates, rendering it one of the most seismically and volcanically active places globally. This tectonic situation renders the majority of Indonesia's coastal regions highly susceptible to earthquakes and tsunamis. The Sunda Strait Segment, a component of the Sunda megathrust subduction system, possesses the capacity to produce significant tsunamis. This region has historically been devoid of significant energy release manifested in major earthquakes, so specialists refer to it as a seismic gap [1]. Seismotectonic studies predict that the maximum potential magnitude in this segment might reach $M_w$ 8.7 [2], which, if realized, has the capacity to produce a tsunami of considerable height and inundation range.

The Palabuhanratu Bay region, situated on the southern coast of West Java Province, is one of the regions directly bordering this subduction zone. This location possesses distinctive geographic features, including a semi-enclosed bay, a sinuous shoreline, and mountainous terrain in the northern area. Palabuhanratu has changed from a residential suburb to a coastal tourist spot that gets a lot of visitors, especially during the holidays [3]. With a lot of tourists in the area and being physically exposed, this situation increases the chance of a tsunami occuring.

Indonesia's coastal regions have come up with a number of ways to lessen the damage, such as setting up early warning systems, evacuation routes and sites, and programs to get people involved in their communities. Nevertheless, other areas, including Palabuhanratu, continue to experience deficiencies in evacuation infrastructure, community responsiveness, and the application of cost-effective and rapidly deployable local solutions. Therefore, making sure that communities are ready for a tsunami is important for lowering the number of deaths that could happen.

This study aims to evaluate the tsunami hazard level in the Palabuhanratu Bay area through numerical simulations that generate tsunami heights, arrival times, and inundation areas. Based on the simulation results, evacuation route optimization was conducted using Dijkstra's algorithm to determine the fastest route to a safe area. Furthermore, this article proposes a community-based mitigation innovation, namely the placement of life buoys along the coastline and evacuation routes as a means of escape for residents and tourists in the event of a tsunami. This approach is expected to be a low-cost, easy-to-implement, and relevant mitigation solution for coastal areas with limited resources like Palabuhanratu.

## 1.1. Tsunami Hazard in the Sunda Strait Region

The Sunda Strait area is recognized as one of the most active subduction zones in Indonesia, where the Indo-Australian Plate subducts beneath the Eurasian Plate at an average pace of 6–7 cm annually. Historical records indicate numerous significant earthquakes and tsunamis resulting from this tectonic interaction, notably the 1883 eruption of Krakatoa and the 2018 collapse of the Anak Krakatau region, both of which produced devastating tsunamis impacting the adjacent beaches of Java and Sumatra.

Numerous studies have simulated the possibility of a tsunami generated by a megathrust subducting beneath the Sunda Plate. Modeling by Supendi et al. predicts that a megathrust earthquake with a magnitude of Mw 8.9 might produce a tsunami with a maximum wave height of approximately 34 m over the west coast of southern Sumatra and the south coast of Java at the Ujung Kulon Peninsula [4]. These findings indicate that the Palabuhanratu Bay area, which is directly in front of the subduction front, is one of the places that is probably to be hit by a tsunami and has inadequate natural protection.

### 1.2. Coastal Vulnerability and Tourism Exposure

Coastal tourism areas often face a dual challenge: they are both economically vital and physically vulnerable. High visitor density, seasonal population fluctuations, and limited local knowledge about disaster risks can exacerbate the impacts of tsunamis. A study by Gulo and Koestoer [5] looked at how New Zealand and Indonesia handle coastal tourism during natural disasters. New Zealand has built a good early warning system and made the public more aware, instead Indonesia has challenges managing natural disasters because of its large area and lack of financial resources. His research suggests creating a better early warning system, giving tourism operators better safety training, and giving disaster mitigation greater resources, especially in coastal areas. These steps are meant to make Indonesia better able to deal with possible natural disasters [5].

In the case of Palabuhanratu, the coastal morphology—a semi-enclosed bay with steep hinterlands—creates additional challenges for evacuation and dissipating tsunami run-up. Previous assessments by BNPB [6] identified this bay as a high-risk tsunami-prone zone, emphasizing the need for tailored preparedness strategies that integrate both permanent residents and temporary visitors.

### 1.3. Simulation and Modeling Approaches for Tsunami Hazard Assessment

Tsunami hazard assessment typically involves numerical simulations using shallow water equations or non-linear wave propagation models to estimate parameters such as wave height, arrival time, and inundation extent. Tools such as MOST, TUNAMI-N2, and COMCOT [7,8] can be said to be the pioneers of numerical tsunami modeling. Later, other software such as VOLNA, NAMI-DANCE, FPGA, TIMPULSE-SIM, and Delft3D [7,9–12] were developed which are widely used to model the propagation of tsunamis and run-up along complex coastlines. Tsunami models emphasize that local topography, bathymetry, and coastal configuration strongly influence inundation depth and arrival time [13]. This work utilizes numerical modeling to analyze tsunami behavior in Palabuhanratu Bay, generating hazard maps that serve as a foundation for evacuation planning. The application of such models facilitates a more precise assessment of community exposure zones and probable safe evacuation places.

#### 1.3.1. Evacuation Route Optimization

Effective evacuation planning is critical to reducing fatalities during tsunami events, especially when the warning-to-arrival time is limited. The Dijkstra algorithm, a well-known graph-based optimization method, has been extensively applied in spatial decision-making and shortest-path analysis [14]. Previous works [15–18] have demonstrated its applicability in determining optimal evacuation routes in complex urban and coastal terrains. The algorithm utilizes topography data, land use, and road networks to determine the shortest or fastest paths to designated safe zones. In Palabuhanratu, where the topography varies sharply from coastal lowlands to elevated hills, this approach provides a quantitative basis for identifying optimal evacuation routes within the constrained timeframe preceding tsunami impact.

#### 1.3.2. Community-Based and Low-Cost Mitigation Strategies

Recent disaster management paradigms highlight the importance of community-based approaches that empower local residents to take proactive roles in disaster preparedness. Combining local wisdom with low-cost technologies can significantly improve survival rates during disasters [19]. One such innovation was inspired by lessons from previous tsunamis (e.g., 2004 Indian Ocean tsunami). In addition, many survivors reported clinging to floating debris to survive after being swept away by tsunami waves, as in the Palu Tsunami and Sunda Strait Tsunami, both of which occurred in 2018 [20–22]. Hence, integrating floating safety equipment along evacuation routes and coastal areas could provide an additional layer of protection, especially in regions where vertical evacuation structures are limited.

#### 1.3.3. Summary of Key Findings from Literature

The reviewed studies collectively underscore three essential points: 1) The Sunda Strait segment poses a high tsunami hazard with the potential to impact Palabuhanratu Bay severely; 2) Tourism-driven coastal areas require specialized preparedness strategies that account for transient populations and limited infrastructure; 3)The integration of numerical simulation, route optimization, and community-based innovations offers a promising pathway for enhancing tsunami resilience at the local scale. Building upon these insights, the present study focuses on quantifying the tsunami hazard in Palabuhanratu Bay, optimizing evacuation routes, and proposing an innovative, low-cost mitigation concept through community-based deployment of life buoys along vulnerable coastal zones.

## 2. Methods

This section delineates the methodologies employed in this investigation. Numerical models of tsunami propagation were conducted with the earthquake's epicenter situated in the Indian Ocean. The evacuation routes and lifebuoy placement strategies were subsequently examined.

### 2.1. Study Area

The study is carried out in Palabuhanratu Bay, positioned on the southern coast of West Java, Indonesia, approximately 120 km southwest of Bandung (**Figure 1**). The bay directly confronts the Sunda Strait subduction front and features a semi-enclosed shape, typified by high hills to the north and narrow coastal plains along the shoreline. The area operates as a fishing town and a seaside tourism hub, drawing thousands of visitors each year. This bay area contains the Ciletuh–Palabuhanratu UNESCO Global Geopark, recognized by UNESCO for its significant potential as a coastal tourism destination. It has been identified as one of the nine premier tourism sites in West Java Province due to its distinctive location and high tourist visitation rates [23]. Geographically, the study area extends from 6°58′S to 7°02′S and from 106°29′E to 106°35′E. Palabuhanratu has been classified as a high tsunami risk zone by Indonesia's National Disaster Management Agency (BNPB) due to its topography and significant population exposure [6].

### 2.2. Research Framework and Data Collection

The research methodology comprises three major stages: 1) tsunami simulation and hazard assessment, 2) evacuation route optimization, and 3) community-based mitigation concept development. Each stage is designed to sequentially build an integrated understanding of tsunami hazard, evacuation feasibility, and local preparedness enhancement. Several datasets were used to support the simulation and spatial analysis, as summarized in **Table 1**.

All spatial datasets were processed and integrated into a Geographic Information System (GIS) environment.

### 2.3. Tsunami Numerical Simulation

The tsunami propagation and inundation were simulated using a hydrodynamic model based on the nonlinear shallow water equations (NSWE), which govern mass and momentum conservation for long-wave propagation. The equations were solved numerically using a finite difference scheme on a nested grid to capture nearshore wave transformation accurately. Boundary conditions were defined by the initial sea surface displacement derived from the earthquake source parameters following the Okada elastic dislocation model. Bathymetric data is necessary for the tsunami propagation model from the source to sites evaluated. Batnas (6 arcsec resolution) bathymetry data are used in this investigation. The Geospatial Information Agency, or BIG in Indonesian, is the source of these data. The simulation layer was formed using bathymetry data. Three simulation layers that make up a layered grid system are used in this investigation. Numerical equations are solved in this work utilizing explicit staggered leap-frog finite difference techniques in COMCOT [8]. The simulation outputs included: wave height at selected observation points, arrival time (ETA) of the first wave, and inundation extent and depth within the coastal plain. Model validation was performed by comparing simulation results with available historical tsunami records and topographic consistency checks.

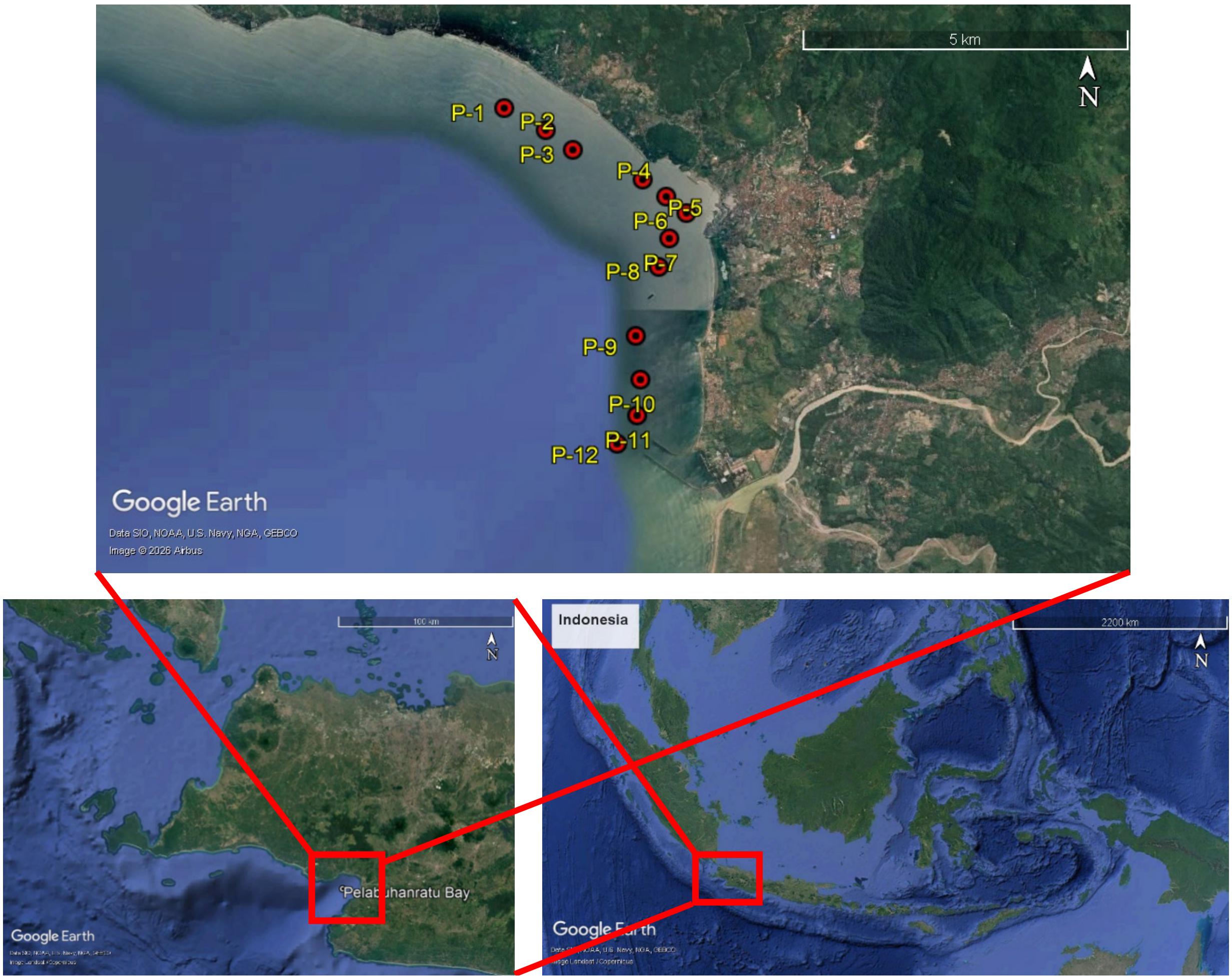


**Figure 1.** Palabuhanratu Bay is located on the southern coast of West Java Province, facing the Indian Ocean, where the megathrust is the source of the earthquakes. Symbols P-1–P-12 are observation points.

**Table 1.** Data type and source.

| Data Type | Description | Source |
|---|---|---|
| Bathymetry and topography | Data Digital Bathymetry Model (Batnas) with 6 arc sec resolution. | Geospatial Information Agency (BIG). |
| Seismic source parameters | Fault geometry, slip rate, and magnitude scenario (Mw 8.7). | Indonesian Agency for Meteorological, Climatological and Geophysics (BMKG), National Earthquake Study Center (Pusgen). |
| Land use and infrastructure | Roads, buildings, and open spaces. | Regional Development Agency (Bappeda Sukabumi Regency). |
| Population and tourism data | Distribution of residents and tourist accommodation. | Local government statistics. |
| Observation points | 12 control points across the bay area. | Field survey and GIS digitization. |

## 2.4. Evacuation Route Optimization

An examination of evacuation routes was performed utilizing the Dijkstra shortest-path algorithm, which determines the minimum-cost path from an origin (observation point) to a destination (safe zone) inside a weighted network. The standard protocol comprises:

a. Network creation—Road networks and walkways were digitized from satellite data and allocated travel speeds based on slope and surface classification.
b. Cost weighting—Each segment was assigned a weight based on walking speed (m/s), terrain gradient, and possible impediments.
c. Identification of safe zones—Areas elevated above 20 meters from mean sea level were designated as safe zones according to simulation outcomes.
d. Path computation—The Dijkstra algorithm, implemented through scripting in the GIS environment, determined the ideal evacuation routes and calculated trip durations.
e. Scenario evaluation—Various routes (including alternates for each observation location) were assessed to provide redundancy across diverse road accessibility scenarios.

The resulting evacuation maps visualize the optimal paths, estimated travel times (in minutes), and distances (in meters) for each populated and tourist cluster. The data used to design the route is the distance data between nodes, which in this study was selected from Google Maps. After that, it continued by determining the weight of each node based on the distance. Evacuation routes that use roads must be paved at least with unsealed pavement such as Telford roads, gravel roads, and densely packed dirt roads, in accordance with the technical planning, principles of evacuation routes in the Tsunami Natural Disaster Evacuation Route Planning Guidelines of the Directorate General of Highways [24]. The number of evacuation routes can be determined by the formula:

$$N_r = \frac{P}{Q \ x \ t_E} \quad (1)$$

where $N_r$: number of evacuation routes; $P$: Projected number of affected residents (people); $Q$: ideal evacuation route capacity (people/minute); $t_E$: evacuation time (minutes)

Evacuation distance can be calculated using:

$$S = V_E \ x \ t_E \quad (2)$$

where $S$: evacuation distance; $V_E$: speed of the person moving (m/min)

Evacuation time is formulated:

$$t_E = t_B - t_P - t_R \quad (3)$$

where $t_B$: estimated time of tsunami arrival (minutes); $t_P$: warning time (minutes); $t_R$: community reaction time (minutes)

Dijkstra's algorithm focuses on finding the path with the lowest cost between one point and another. The end result of the algorithm is finding the shortest path based on the smallest weight from one point to another.

## 2.5. Community-Based Mitigation Strategy

Subsequent to the simulation and evacuation assessments, a low-cost and community-based mitigation strategy was proposed. The concept emphasizes the deployment of life buoys (floating rescue devices) throughout essential coastline areas and adjacent to evacuation routes. The idea is based on factual observations indicating that numerous tsunami survivors have depended on floating objects for survival during wave run-up incidents.

The deployment density of life buoys was established by integrating the inundation map with population exposure data. Increased densities were suggested in proximity to heavily populated coastal areas and at the entrances of evacuation routes. Community involvement is promoted in the upkeep, training, and functioning of these devices, thereby cultivating a culture of local readiness and collective accountability.

## 2.6. Methodological Assumptions and Limitations

Several simplifying assumptions were made to ensure computational feasibility: 1) The tsunami source was modeled as a single-fault rupture event representing the worst-case scenario (Mw 8.7); 2) Structural resistance of buildings and vegetation friction were not explicitly modeled; 3) Human behavior variability during evacuation (e.g., panic, decision delay) was represented by average walking speeds (1.0–1.2 m/s); 4) The sensitivity analysis of evacuation route selection is only based on the walking speed factor of residents, without considering other factors that also influence route selection such as distance, number of people, age, and weather.

A worst-case scenario simulation method is implemented with the most influential parameters: an earthquake magnitude of Mw 8.7 and an epicenter location at 104.547612°E and −7.277303°S. These magnitudes were taken from the earthquake hazard map published by the National Earthquake Study Center (Pusgen), while the epicenter was chosen in the middle of the megathrust segment closest to the study location, namely the Sunda Strait megathrust. With the epicenter located around the middle of the megathrust segment, the length and width of the earthquake rupture area are still within the Sunda Strait megathrust segment. The length and width of the rupture area is estimated using the scaling relation proposed by Wells and Coppersmith [25] and Blasser et al. [26]. The image of the Sunda Strait segment can be seen in the **Figure A.2** (**Appendix A**).

Furthermore, the southern region of Java is frequently detected as experiencing "tsunami earthquakes," such as those seen in the 1992 and 2006 Java Tsunamis. This type of earthquake has a complex mechanism due to its slow rupture time. COMCOT, on the other hand, has limitations in this regard because the rupture is calculated to occur instantaneously. Despite these limitations, the methodology provides a robust basis for assessing tsunami hazard, evacuation feasibility, and low-cost mitigation strategies applicable to similar coastal settings in Indonesia.

# 3. Results and Discusion

## 3.1. Tsunami Propagation and Inundation

For the model input in this study, the earthquake epicenter is assumed to be located around the middle of the Sunda Strait megathrust segment, where, in this simulation, the epicenter is taken at 104.547612 E and –7.277303 S. Other parameters inputted in the model include focal depth (20 km), fault length (388 km), fault width (139 km), strike angle (300°), dip angle (45°), slip angle (100°), and slip (8.75 m). The results of the numerical simulation indicate that the potential for an earthquake with a magnitude of Mw 8.7 originating from the Sunda Strait megathrust segment will generate significant tsunami waves that reach the southern coast of West Java, including Palabuhanratu Bay. **Figure 2** illustrates the simulation of tsunami wave propagation entering the Palabuhanratu Bay area. Approximately 10–12 min after the earthquake occurred, the tsunami began to enter the bay (**Figure 2a,b**). At 15–17 min, some parts of the bay's shoreline experienced a water level rise of nearly 5 m (**Figure 2c,d**). Furthermore, at 20 min, all shorelines in the bay experienced a water level rise above 5 m. Finally, at 21–22 min after the earthquake, the edge of the bay had reached the peak of the tsunami wave (**Figure 2e,f**). Wave energy was focused into the semi-enclosed bay due to refraction and the coastal configuration.

For more detailed attention, the end of the bay was reviewed by placing numerical observation points at places known to the community or tourists, where 12 observation points were taken, namely P-1 to P-12. The graph of changes in sea level elevation, in this case showing the amplitude and height of the tsunami, is presented in **Figure 3**. The crest of the first tsunami wave is estimated to arrive approximately 21–23 min after the initial earthquake. Analysis of wave amplitudes at 12 observation points around the bay shows maximum wave heights ranging from 7 to 10 m, which classifies the event as a large tsunami according to the hazard category [27].

The affected area can be understood in greater detail by combining simulation data with satellite imagery. **Figure 4a** detects the coastal areas hit by the tsunami, where the results were taken when the tsunami peak reached the end of the bay, shown in red. Tsunami run-up can cause inundation. To determine the inundation that occurred in this area, the tsunami waves were separated and only taken on the land side so that the inundation area could be detected, as shown in **Figure**

**4b**. The inundation area is estimated to reach 15 km$^2$ for the area around the end of the bay alone, primarily affecting the flat coastal plains near the Palabuhanratu Fish Landing Base, the main market area, and several popular tourist beaches. The maximum inundation distance to land reaches 450–700 m. In this study, no hydrodynamic tsunami run-up simulation was conducted, so the direction and speed of run-up on land are unknown. If this is to be simulated, high-resolution topography data will be required.

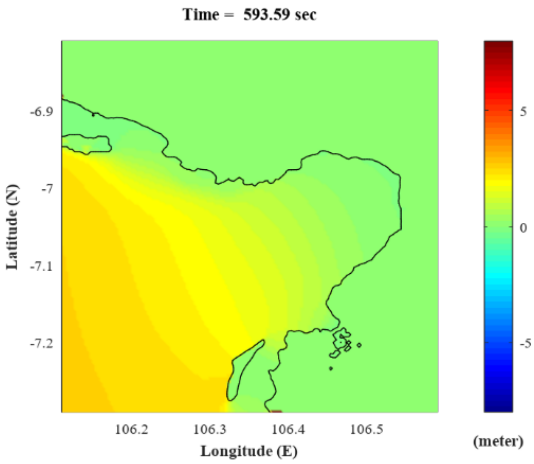


(**a**) Tsunami propagation ≈10 min after an earthquake.

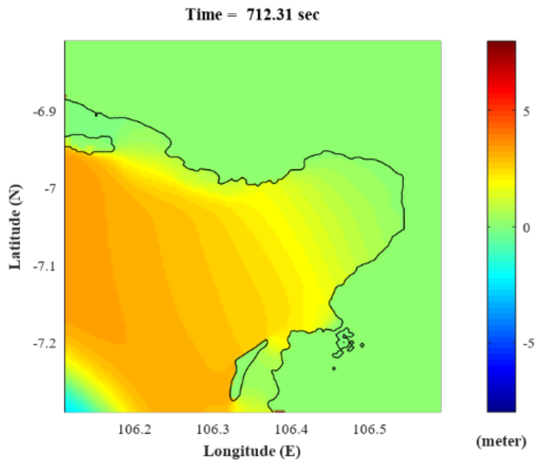


(**b**) Tsunami propagation ≈12 min after an earthquake.

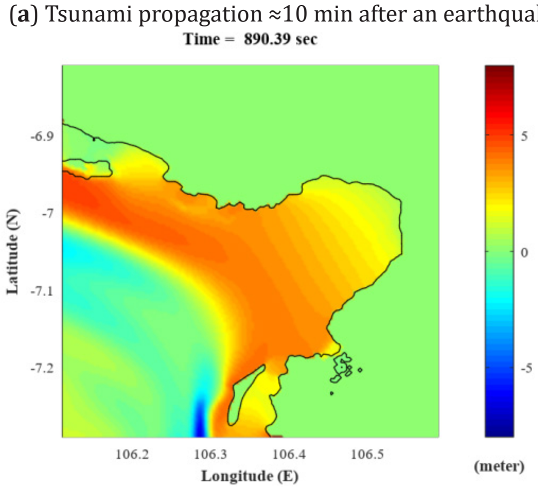


(**c**) Tsunami propagation ≈15 min after an earthquake.

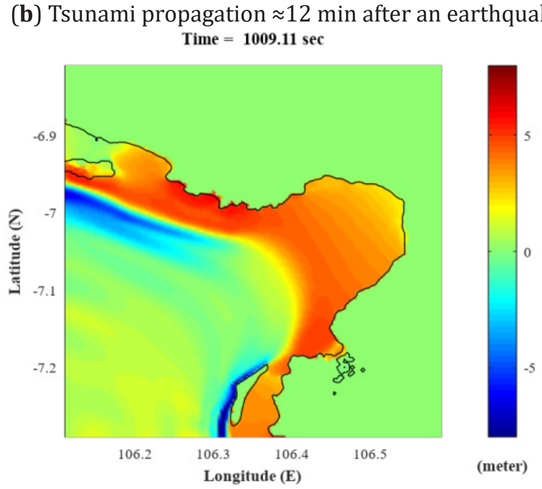


(**d**) Tsunami propagation ≈17 min after an earthquake.

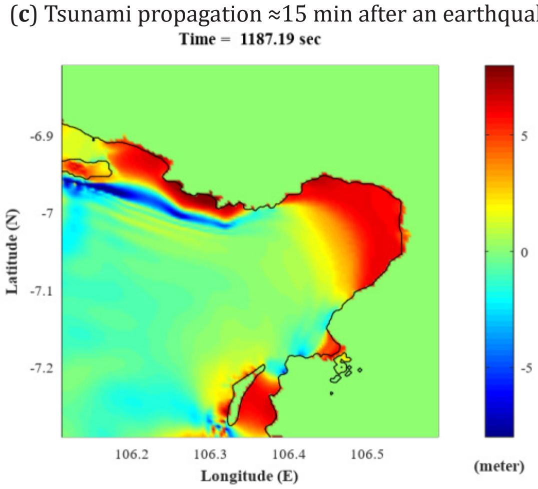


(**e**) Tsunami propagation ≈20 min after an earthquake.

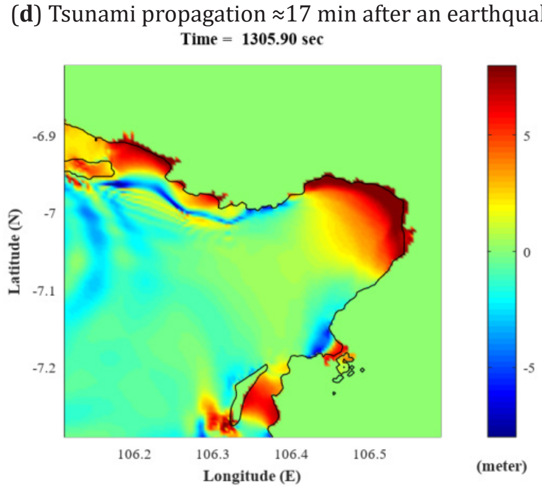


(**f**) Tsunami propagation ≈22 min after an earthquake.

**Figure 2.** Tsunami simulation results in a 2-D view.

Note: The tsunami reached the Palabuhanratu Bay after traveling from the source of the earthquake in the Indian Ocean.

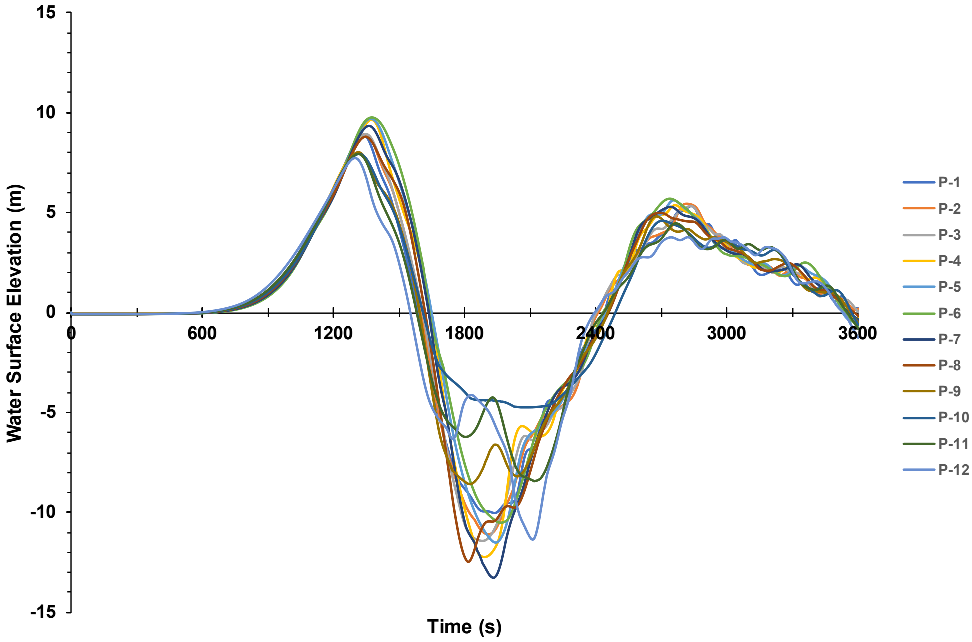


**Figure 3.** The simulation results take the form of a rise in the water level due to the tsunami at several observed points in Palabuhanratu Bay.

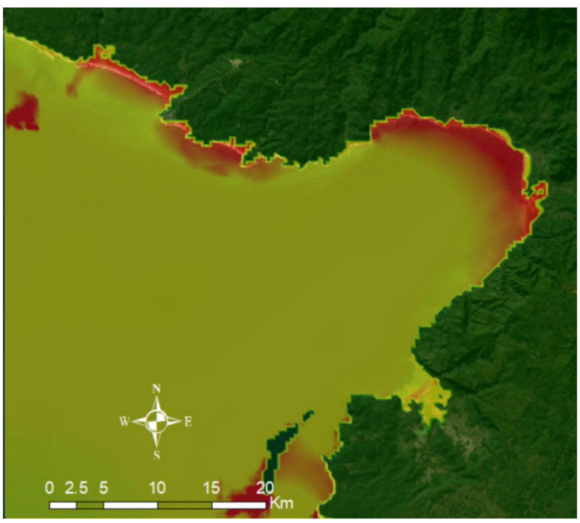


(**a**) Tsunami reaches coastline of Palabuhanratu Bay.

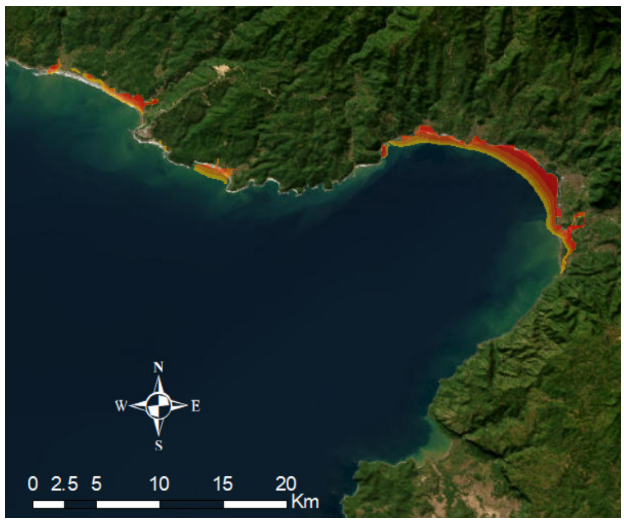


(**b**) Tsunami inundation area.

**Figure 4.** Tsunami impacted area and inundation in Palabuhanratu Bay were detected by simulation data combined with satellite imagery.

Based on the simulation outputs, the spatial distribution of tsunami hazard levels, the tsunami hazard in Palabuhanratu Bay was classified into three categories:

- High hazard zone: areas with inundation depth >3 m and velocity >2 m/s, primarily along the coastal settlements and tourist beaches.
- Moderate hazard zone: inundation depth 1–3 m, generally affecting the lower parts of road networks and open areas near the harbor.
- Low hazard zone: inland areas above 20 m elevation, identified as potential safe zones for vertical or horizontal evacuation.

**Figure 4** presents the inundation areas. It shows that approximately 63% of the urbanized coastal area falls within the high hazard category, underscoring the urgency for well-defined evacuation routes and rapid response mechanisms. This spatial quantification provides an essential basis for land-use planning and community preparedness training.

## 3.2. Evacuation Route Optimization

The Dijkstra algorithm successfully generated several alternative evacuation routes from each of the 12 observation points to the designated safe zone. **Table 2** presents the observation locations, focusing on the tip of Palabuhanratu Bay, along with related information such as longitude, latitude, potential tsunami amplitude, and estimated arrival time. In total, 20 optimal routes were identified from the 12 observation locations, with a relatively uniform potential tsunami amplitude of 8–9 m and an estimated average travel time of 22–23 min. The amplitude and arrival time were obtained from simulation results, the graph of which is shown in **Figure 2**.

**Table 2.** List of observation points.

| Site | Longitude | Latitude | Description | Potensial Tsunami Amplitude (m) | Estimated Time Arrival (min) | Evacuation Time (min) |
|---|---|---|---|---|---|---|
| P-1 | 106.513241 | −6.973466 | South of Dolphin Beach and Citepus Beach | 8.89 | 22.61 | 16.61 |
| P-2 | 106.519045 | −6.976478 | South of Citepus Beach | 8.91 | 23.32 | 17.32 |
| P-3 | 106.522836 | −6.979185 | South of Pati Padi Beach, Ciletuh Geopark Information Center, Palabuhanratu, and Citepus Park | 8.92 | 23.56 | 17.56 |
| P-4 | 106.532569 | −6.983218 | South of Palabuhanratu Presidential Palace Beach | 9.64 | 23.85 | 17.85 |
| P-5 | 106.535867 | −6.985562 | South southwest of New Pier, Bayu Amrta Hotel, and Karang Sari Beach | 9.69 | 23.91 | 17.91 |
| P-6 | 106.538697 | −6.987826 | Southwest of Gadobangkong Square, Ciletuh Geopark and Bali Transportation Fish Auction Place (TPI), northwest of Nusantara Fisheries Port (PPN), and west of Pier 1 Palabuhanratu | 9.75 | 23.67 | 17.67 |
| P-7 | 106.536362 | −6.991393 | West of the Nusantara Fisheries Port and Palabuhanratu Pier 2 | 9.33 | 23.38 | 17.38 |
| P-8 | 106.534959 | −6.995396 | The west of Palabuhanratu Beach | 8.79 | 22.85 | 16.85 |
| P-9 | 106.531893 | −7.005065 | West of the coast, the Fisheries Training Bureau, LPK Mutiara Sagara, PT Jawa Suisan Indah, and PT AFI Lautan Indonesia | 8.01 | 22.50 | 16.50 |
| P-10 | 106.532607 | −7.011161 | West of Twenty Cipatuguran Beach and surrounding residential areas | 7.93 | 22.26 | 16.26 |
| P-11 | 106.532208 | −7.016177 | Northwest of Kampung Perahu Jayanti Beach | 7.93 | 22.26 | 16.26 |
| P-12 | 106.529492 | −7.020168 | West of the Palabuhanratu PLTU, GIs Palabuhan Ratu, and the Palabuhanratu Ship Unloader | 7.72 | 22.08 | 16.08 |

The inundation area obtained from the inundation map is estimated at 624 ha (6.24 $km^2$). This area is only at the tip of the bay, which is more densely populated and has infrastructure. Outside the tip of the bay, the inundation area due to the tsunami is actually quite significant, with an estimated 20 $km^2$ spread across many areas. The inundated area is considered an affected area that requires the provision of evacuation routes. In this study, evacuation routes are focused on 12 points shown in **Table 2**. The routes are planned for 2030, where the population projection for the next 5 years uses a population growth rate in the Palabuhanratu area of 1.28%. Thus, the projected population until 2030 is 129,453. The prediction for 2030 is divided by the 9460-hectare area of Palabuhanratu District to determine the population density. The population density as a result is 13.68 persons per hectare. Consequently, 8536.32 people are impacted (the result of multiplying the affected area by the population density). There must be at least eight evacuation routes, assuming that ideal evacuation route capacity ($Q$) is 70 persons per minute and that evacuation time ($t_E$) is 17.02 minutes on average.

Evacuation routes were established, including a temporary evacuation location at the end and a beginning point close to the observation point. Popular locations at the end of the bay served as the basis for choosing observation places. As seen from the observation position, the villages of Palabuhanratu, Jayanti, and Citepus were tsunami-affected locations, and these were the Temporary Evacuation Sites (TES). TES were supposed to be constructed in compliance with the recommended height because of flooding, with a focus on public amenities and residential gathering places that could house sizable communities. Emergency evacuation locations that were modified based on the distance reached when the tsunami struck were known as TES. Prior to the Final Evacuation Site (FES), TES were utilized. **Table 3** shows the strategic TES identified using Google Earth. Other sites are given in **Appendix A**, **Table A.1**.

The route from the starting point to the Temporary Evacuation Site passes through numerous nodes, each labeled with letters. These nodes include road bends, T-junctions, intersections, and other important points. **Table 4** lists the node names and descriptions for Route 1 (R-1). Complete data for the other routes is provided in **Appendix A**, **Table A.2**.

It is necessary to determine the distances between nodes on each route. The distances between nodes for routes 1, 3, and 2 are shown in **Table 5** below; **Appendix A, Table A.2** provides the distances for the remaining routes.

**Table 3.** Temporary Evacuation Site (TES).

| Site | Route | Temporary Evacuation Site and Coordinates | Site | Route | Temporary Evacuation Site and Coordinates |
|---|---|---|---|---|---|
| P-1 | R-1 | Islamic boarding school Miftahul Falah (106.525083°, −6.968564°) | P-7 | R-7 | Senior high school SMK Al Fajar Palabuhanratu (106.549106°, −6.991277°) |
| P-2 | R-2 | Yunior and senior high schools: SMP IT Al Fardiyatussaadah, SMAS Islam Al Fardiyatussaadah, MTS Yasfa, Yayasan Panti Asuhan Yasfa (106.532139°, −6.975917°) | P-8 | R-8 | Pasir Honje Settlement (106.544782°, −7.003143°) |
| P-3 | R-3 | Yunior and senior high schools: SMP IT Al Fardiyatussaadah, SMAS Islam Al Fardiyatussaadah, MTS Yasfa, Yayasan Panti Asuhan Yasfa (106.532139°, −6.975917°) | P-9 | R-9 | Settlement of Bukit Ibrahim and Pasir Honje (106.547339°, −7.005819°) |
| P-4 | R-4 | Islamic elementary school SD IT Insan Cendikia, Promotion Building and Development Center Palabuhanratu, senior high school SMKN 1 Palabuhanratu (106.545917°, −6.978593°) | P-10 | R-10 | Rehabilitation social home, elementary school SD Cipatuguran (106.544235°, −7.014844°) |
| P-5 | R-5 | Yunior high school SMPN 3 Palabuhanratu, Promotion Building and Development Center Palabuhanratu (106.546899°, −6.979665°) | P-11 | R-11 | Rehabilitation social home, elementary school SD Cipatuguran (106.545657°, −7.016132°) |
| P-6 | R-6 | Sukabumi Regional Secretary Office, kindergarten TK IT SBB Gema Al Wahid, Sukabumi National Unity and Politics Agency (Kesbangpol), elementary school SDN 3 Palabuhanratu (106.551033°, −6.987704°) | P-12 | R-12 | Rehabilitation social home, elementary school SD Cipatuguran (106.545657°, −7.016132°) |

**Table 4.** Nodes of each route and their description.

| Route | Node | Description | Route | Node | Description |
|---|---|---|---|---|---|
| R-1 | A | Citepus Beach | R-2 | A | Palabuhanratu Beach |
| | B | Gas station of Citepus | | B | Bend in the road |
| | C | Batu Alam Bungalows & Apartment | | C | Parluhutan lodge |
| | D | Building material store Berkah Citepus | | D | Intersection |
| | E | Three-way junction Citepus Cibudus | | E | Three-way junction |
| | J | Small alley | | G | Homestay Syakila |
| | F | Warkop & Sembako 41 | | F | Intersection |
| | G | MI Citepus Hilir | | L | SMP/SMA IT Al Fardiyatussaadah |
| | H | Volleyball court Leotek | | H | Three-way junction |
| | I | Islamic boarding school Miftahul Falah | | I | Bintan travel |
| | | | | J | Three-way junction |
| | | | | K | Citepus Girang complex |
| | | | | M | Yasfa orphanage Foundation |

**Table 5.** Nodes of each route and their distances.

| Route | Node | Distance (m) | Route | Node | Distance (m) | Route | Node | Distance (m) |
|---|---|---|---|---|---|---|---|---|
| R-1 | A–B | 82.09 | R-2 | A–B | 113.90 | R-3 | A–B | 114.44 |
| | B–C | 281.90 | | B–C | 30.00 | | B–C | 33.27 |
| | C–D | 100.48 | | C–D | 89.42 | | B–D | 32.67 |
| | D–E | 40.56 | | D–E | 131.37 | | C–E | 38.41 |
| | D–J | 84.18 | | D–G | 85.64 | | D–E | 35.17 |
| | E–F | 73.43 | | G–F | 102.26 | | E–F | 70.74 |
| | J–F | 71.26 | | E–F | 42.30 | | F–G | 25.23 |
| | F–G | 151.67 | | F–L | 69.75 | | G–H | 42.30 |
| | G–H | 71.89 | | F–I | 104.20 | | H–L | 69.75 |
| | H–I | 80.74 | | G–H | 152.40 | | H–I | 104.20 |
| | | | | H–J | 57.65 | | I–J | 23.67 |
| | | | | I–J | 23.67 | | J–K | 185.13 |
| | | | | J–K | 185.13 | | K–M | 119.10 |
| | | | | K–M | 119.10 | | | |

In creating the shortest route scheme, points (nodes) and networks (linkages) are required to facilitate distance calculations using the Dijkstra algorithm. Nodes can be placed in buildings or structures, and can be placed at road intersections. Meanwhile, linkages are used to connect nodes. The distance between nodes is also measured. In determining nodes, the instrument used is Google Earth. The first step is to add a location marker at the beginning. This starting point is determined by considering the closest initial location from the coast, towards the next point that is increasingly further from the coast. This step is continued until the temporary evacuation site has been determined. For example, at the first point, at observation point 1 (route 1), the Suparman Seafood restaurant, which is the closest point to Citepus Beach, is the starting point. An overview of the routes and their shortest alternative distances (red lines) can be found in **Appendix A, Figure A.1**.

After performing the Dijkstra algorithm calculation, the following is the closest route to the temporary evacuation site at the observation point (**Table 6**).

**Table 6.** Characteristics of representative evacuation routes, including alternatives, shortest routes, and distance.

| Route | Alternatives | Shortest Routes | Distance (m) |
|---|---|---|---|
| R-1 | 1 | A-B-C-D-E-F-G-H-I | 882.76 |
| R-2 | 1 | A-B-C-D-E-F-L | 476.74 |
| | 2 | A-B-C-D-G-H-J-K-M | 833.24 |
| R-3 | 1 | A-B-D-E-F-G-H-L | 390.30 |
| | 2 | A-B-D-E-F-G-H-I-J-K-M | 752.65 |
| R-4 | 1 | A-B-C-D-F-G-H | 854.70 |
| | 2 | A-B-C-D-F-G-I | 946.90 |
| R-5 | 1 | A-B-C-E-G-H-I-J-K-L | 1038.19 |
| R-6 | 1 | A-B-C-D-G-F | 568.80 |
| | 2 | A-B-C-D-G-H-K | 769.96 |
| | 3 | A-B-C-M-O-P-Q-R-T | 889.02 |
| | 4 | A-B-C-M-O-P-Q-S-V | 889.70 |
| R-7 | 1 | A-B-C-E-F-G-H-I-J | 769.87 |
| R-8 | 1 | A-B-C-D-E-F-G-H-I-J | 1322.64 |
| R-9 | 1 | A-B-D-E-F-G-H-I | 995.50 |
| R-10 | 1 | A-G-L-N-P-Q-R-S-V-X-Y-Z-AA | 992.38 |
| R-11 | 1 | A-B-G-H-L-M-N-O | 665.44 |
| | 2 | Y-AA-AB-N-O | 630.61 |
| R-12 | 1 | A-B-H-J | 795.33 |
| | 2 | K-M-O-P-Q-I-J | 885.05 |

The analysis demonstrates that while some routes are short, their effectiveness depends on terrain slope and congestion potential, which is also discussed by Fathianpour et al. [28]. Routes originating near the Palabuhanratu Beach area exhibit shorter distances but require steep uphill movement toward the northern hills, which may reduce effective walking speed. Conversely, routes from Cimaja Beach and Karanghawu Beach are longer but benefit from gentler slopes and more accessible pathways. The simulation of evacuation scenarios reveals that effective evacuation is feasible if initiated within the first 5 min after the earthquake, assuming average walking speeds of 1.0–1.2 m/s. Delays beyond this window would significantly increase exposure to incoming waves. Therefore, early warning dissemination and rapid behavioral response are critical determinants of survival.

Comparison between tsunami arrival time (17–23 min) and estimated evacuation completion time (16–18 min) suggests a narrow safety margin of approximately 2–5 min. This indicates that while evacuation is technically possible, it remains highly sensitive to individual response time and road accessibility. Sensitivity analysis conducted by varying walking speed ±20% shows that even a small delay can reduce survival probability by more than 30%. Consequently, strategies to shorten decision-making time—such as automatic alarm systems, visible signage, and public drills—are essential [29,30]. These findings align with studies by Gowan et al. and Sofyan et al. [31,32], which stress that behavioral readiness often outweighs physical infrastructure in determining survival outcomes.

### 3.3. Community-Based Mitigation: Life Buoy Deployment Concept

This study suggests the installation of floating lifebuoys as an additional mitigation technique, based on empirical evidence that numerous tsunami survivors escaped by clinging to floating debris. The lifebuoys are intended to fulfill dual functions: as safety devices during tsunami run-up and backwash, and as educational icons to enhance public awareness of tsunami hazards. A spatial study integrating population density and inundation likelihood suggests that a provision of 1 lifebuoy per 10 m of coastline over the entire section is likely to ensure sufficient coverage. It is suggested to install additional lifebuoys near evacuation entry points and coastal infrastructure, including lifeguard stations and tourist kiosks. Additionally, lifebuoys are installed at residences along the evacuation path.

Community groups and local lifeguards can play a central role in maintaining these devices and conducting public training on their use. This bottom-up approach aligns with the UNDRR Sendai Framework priorities [33], which emphasize local capacity-building and low-cost innovation in disaster risk reduction. While the system cannot substitute for evacuation infrastructure, it offers a practical, rapidly deployable, and replicable solution for coastal communities with limited resources.

In this context, simple and rapidly deployable community-based mitigation tools are essential. Lightweight emergency flotation devices can help preserve life during tsunami inundation, especially for children, the elderly, or non-swimmers. However, access to commercial life buoys in coastal communities is limited due to cost and distribution constraints. Consequently, low-cost buoy designs using recycled materials—such as plastic bottles, styrofoam, and used drums—have gained interest [34,35], promoting sustainability principles while utilizing abundant coastal waste streams. Based on several surveys and assessments, such as those by Amaratunga et al. [36], plastic waste is abundant in coastal environments and has the potential to become debris. PET bottles are one type of plastic waste that can be used to make lifebuoys. Reusing, recycling, or creatively repurposing materials typically discarded in landfills has become a shared passion for people worldwide. The term “trash to treasure” has become a motto for transforming discarded or unwanted items, often considered trash or waste, into valuable or desirable products [37].

From an engineering perspective, flotation device development requires consideration of material selection, buoyancy performance, structural durability, joint strength, and user ergonomics. The primary principle follows Archimedes’ Law, where buoyant force equals the weight of displaced water (**Figure 5**). Devices should also meet minimum safety requirements related to load capacity and stability in turbulent flow. Strategic spatial distribution along evacuation routes (**Figure 6**)—such as routes leading inland and toward vertical shelters—can increase accessibility during emergency movement.

This study developed a simple square flotation board (60 × 60 × 9 cm) using recycled rubber foam sourced from mattresses and protective packaging waste (**Figure 7**). Rubber foam was selected for its natural buoyancy, elasticity, and cost efficiency. Laboratory and limited field testing assessed buoyancy capacity, static load performance, and user comfort using proxy weights (40–70 kg). Results indicate the device provides adequate support for individuals weighing below 50 kg or as a partial flotation aid when supporting the chest or abdomen. For users above 60 kg, increasing volume or combining multiple units is recommended (**Figure 8**).

Comparative evaluation with other types of flotation materials was conducted, including recycled styrofoam, plastic bottles, and commercial EVA/PVC devices (**Table 7**). Rubber foam demonstrates intermediate performance: more durable and comfortable than styrofoam, but with lower buoyancy per unit volume; and less capable than commercial products, but substantially more affordable and accessible. A modular configuration—attaching two or more boards—can improve buoyancy to adult requirements.

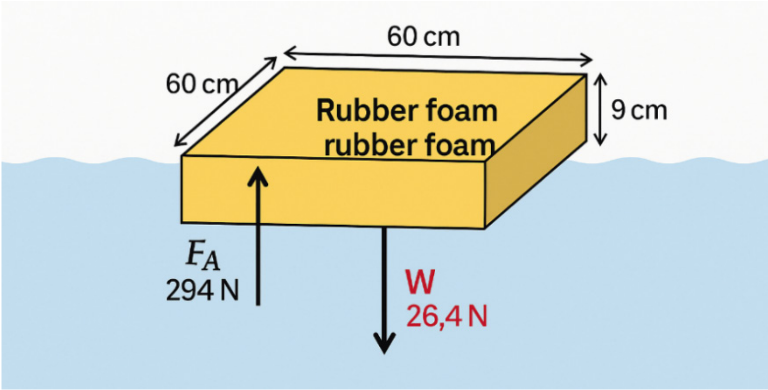


**Figure 5.** Illustration of buoyancy based on Archimedes' law.


**Figure 6.** Evacuation route R-1, lifebuoys need to be increased around the route, and can be installed on buildings or houses.

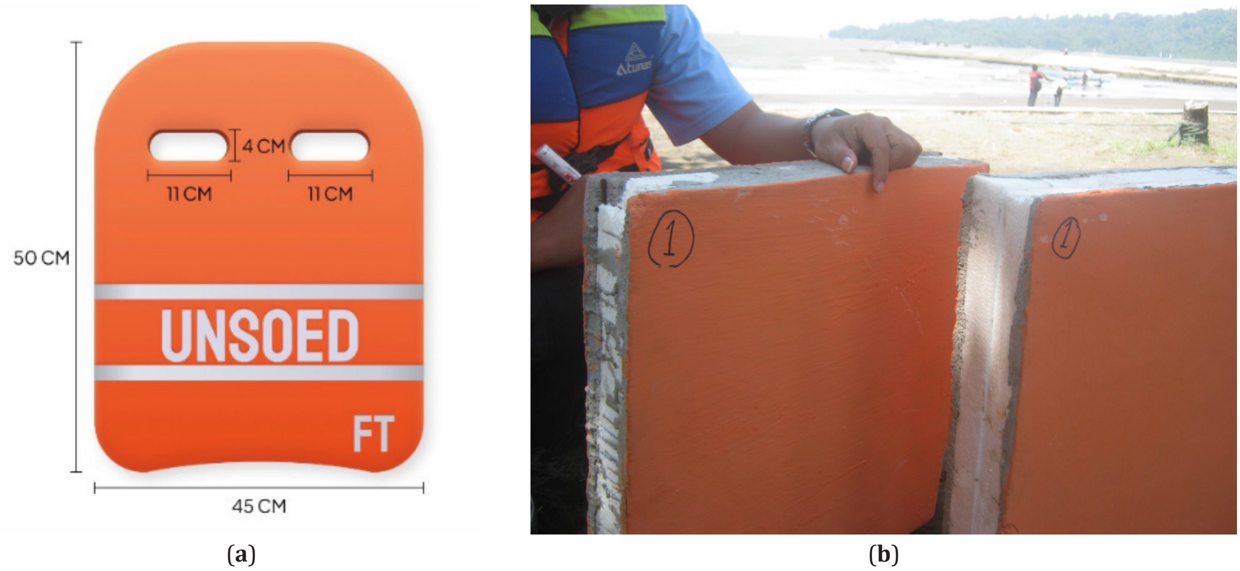


**Figure 7.** Designs and prototypes of floating objects being developed for emergency rescue from tsunamis: (**a**) A design for a prototype buoy made of rubber foam/sponge rubber; (**b**) Wall panels made of styrofoam on the inside and a thin layer of concrete on the outside.

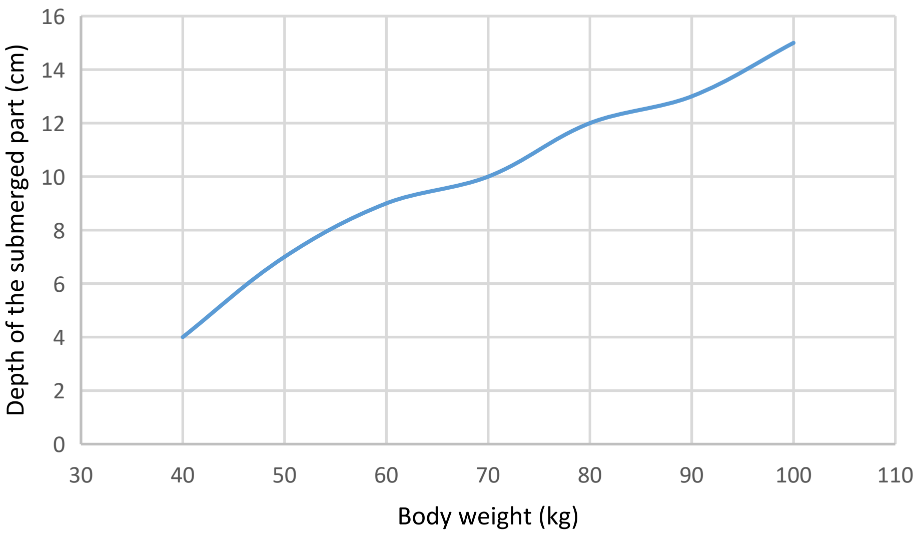


**Figure 8.** The relationship between body weight and the depth of the submerged part of the float.

**Table 7.** Comparison of 4 types of floats.

| Type of Buoy ($m^3$) | Volume ($m^3$) | Self Weight (kg) | Maximum Load (kg) | Advantages | Disadvantages |
|---|---|---|---|---|---|
| Rubber Foam | 0.0324 | 3.88 | ±28.5 | Durable, flexible, and stable | High self-weight, moderate buoyancy |
| Styrofoam | 0.030 | 0.90 | ±29.0 | Lightweight, highly buoyant | Fragile, easily crushed |
| Used Plastic Bottles | 0.015 | 0.60 (8 bottles) | ±12–15 | Inexpensive, waterproof, readily available | Difficult to assemble, non-ergonomic shape |
| Commercial EVA/PVC | 0.04–0.06 | 1.5–2.0 | 70–90 | Ergonomic, strong, and meets safety standards | Expensive, requires special fabrication |

Overall, recycled rubber foam flotation pads represent an effective, low-cost, community-driven innovation aligned with blue-economy and circular material principles. Further design optimization—such as protective coatings, layered volume expansion, and integration with wall-mounted emergency panels—can enhance suitability for broader tsunami preparedness applications. Industry plays a crucial role in developing more reliable lifebuoys, as does the government's regulatory role. A study by Rahmafitria et al. [38] on disaster management in Indonesian tourist destinations suggests that synergy between the community, industry, and government is essential for building resilient communities. However, they also caution that inadequate institutions can hinder collaboration and reduce community resilience. Collaborative models operate effectively when formal institutions act as primary coordinators and ensure transparency, decision-making, and representation. Furthermore, communities and formal educational institutions are crucial as foundations for building community resilience.

### 3.4. Discussion of Findings

The integrated results reveal that Palabuhanratu Bay faces a significant tsunami threat, yet opportunities exist to enhance resilience through spatial planning, optimized evacuation design, and low-cost innovations. Key insights include: 1) The bay's topographic confinement amplifies tsunami energy, increasing localized wave heights; 2) Evacuation feasibility remains marginal due to short warning times and terrain constraints; 3) Hybrid mitigation approaches, combining numerical modeling with community engagement, yield the most sustainable outcomes. The significant tsunami threat stated in this study is in line with the investigation by Setyonegoro et al. [39], which revealed that, in addition to the megathrust, there is a potential tsunami impact in the Palabuhanratu Bay area caused by a combination of local earthquakes and underwater landslides around the bay.

This study contributes to the growing body of literature emphasizing localized, data-driven preparedness strategies for tsunami-prone tourism areas. It demonstrates that advanced modeling and optimization methods can directly inform practical, community-scale interventions, bridging the gap between scientific assessment and real-world implementation. Lifebuoys are an individual endeavor, but that doesn't mean the human body can withstand the enormous force of tsunami waves. For example, post-tsunami field investigations in Palu Bay identified a 54-ton bridge that was displaced nearly 10 m by a 3–4 m tsunami [20]. Therefore, the use of lifebuoys must be accompanied by individual skills while floating in creeping water. While the concept needs to be refined, the results of this study support the goal of achieving zero casualties if tsunami preparedness can be implemented, encompassing both horizontal and vertical evacuation, as discussed by Bernard [40].

## 4. Conclusions and Recommendations

### 4.1. Conclusion

This study explored tsunami preparedness in the coastal tourism region of Palabuhanratu Bay, West Java, incorporating numerical simulation, evacuation route optimization, and community-based mitigation strategy. The principal conclusions can be summarized as follows:

1. Tsunami hazard: A megathrust earthquake with a magnitude of Mw 8.7 originating from the Sunda Strait segment would produce tsunami wave heights of 7–10 m at Palabuhanratu Bay, arriving 17 to 23 min post-shock. The anticipated inundation area covers approximately 6.24 $km^2$, indicating a major tsunami category.
2. Evacuation feasibility: An investigation of evacuation routes utilizing the Dijkstra algorithm revealed 20 ideal pathways linking populous and tourist regions to safe zones situated above 20 m in elevation. The typical evacuation duration ranges from 16 to 18 min, resulting in a limited safety margin of 2 to 5 min prior to wave arrival.
3. Preparedness challenges: The limited warning-to-arrival time and constrained topography highlight the need for rapid decision-making and locally adapted evacuation strategies. Behavioral readiness and early warning dissemination are decisive factors in survival probability.
4. Innovative mitigation: The proposed life buoy deployment system represents a simple yet effective community-based mitigation concept. This strategy enhances the culture of self-rescue and resilience in resource-constrained coastal regions by supplying accessible floating rescue devices and involving local inhabitants in preparedness initiatives.

This study illustrates that the integration of hydrodynamic modeling, geographical optimization, and social innovation offers a comprehensive framework for improving tsunami preparedness in coastal tourism areas. The results are applicable to other coastal areas experiencing analogous geological and socio-economic circumstances throughout Indonesia and the wider Indo-Pacific region.

### 4.2. Recommendations

Based on the results and implications of this study, several recommendations are proposed for future policy and research directions:

1. Policy integration: Local governments should incorporate tsunami hazard maps and evacuation route information into spatial and tourism development planning, ensuring that essential infrastructure and tourist amenities adhere to disaster-resilient design standards.
2. Early warning enhancement: The short interval between earthquake occurrence and tsunami arrival requires the strengthening of local early warning systems, such as automated alerts, coastal sirens, and mobile-based notification networks connected to BMKG data.
3. Public education and drills: Regular evacuation drills and awareness campaigns should be institutionalized in partnership with schools, community organizations, and tourism operators to reduce decision-making delays during emergencies.
4. Infrastructure improvement: Where practicable, vertical evacuation structures or secure shelters ought to be constructed in high-risk areas, especially in regions where evacuation duration surpasses 18 min.
5. Further research: Subsequent investigations may enhance tsunami hazard modeling by integrating structural resilience, vegetation resistance, and behavioral simulations, while also examining multi-hazard preparedness frameworks that encompass tsunami, storm surge, and coastal erosion concerns. In addition, a more in-depth sensitivity analysis of evacuation route selection is necessary. This analysis should be conducted not only by varying walking speed but also by varying the route itself. The route has the highest sensitivity to changes in several parameters, such as walking speed, distance, number of people, weather, age group, and other parameters. Based on this, it will be possible to determine which routes should be provided with more lifebuoys or which routes are designated for the elderly or people with disabilities. Furthermore, to obtain information about the likelihood of a smaller-scale tsunami, a probabilistic tsunami hazard assessment (PTHA) approach can be implemented.

This research translates scientific analysis into tangible initiatives, thereby contributing to the national and regional aim of "Building Coastal Resilience through Blue Economy and Sustainable Tourism." The experience from Palabuhanratu Bay may act as a reference model for other Indonesian coastal communities in pursuing safer and more resilient futures.

## Author Contributions

Conceptualization, W.W. and S.N.P.; methodology, W.W. and S.N.P.; software, W.W., S.N.P., A.N.L.B.Z., A.M.R., and H.F.R.; validation, W.W., S.N.P., and M.A.I.; formal analysis, W.W., S.N.P., M.A.I., A.N.L.B.Z., and A.M.R.; investigation, A.M.R., A.N.L.B.Z., H., and M.W.Z.A.A.; resources, W.W., S.N.P., and A.M.R.; data curation, A.M.R., A.N.L.B.Z., H., and M.W.Z.A.A.; writing—original draft preparation, W.W.; writing—review and editing, W.W., S.N.P., and M.A.I.; visualization, S.N.P., M.A.I., A.N.L.B.Z., A.M.R., and H.F.R.; supervision, W.W. and S.N.P.; project administration, A.N.L.B.Z. and H.F.R.; funding acquisition, W.W. All authors have read and agreed to the published version of the manuscript.

## Funding

This work was supported by Universitas Jenderal Soedirman grant number 14.395/UN23.34/PT.01/V/2025.

## Institutional Review Board Statement

Not applicable.

## Informed Consent Statement

Not applicable.

## Data Availability Statement

Data are available on request.

## Acknowledgments

The authors are grateful for the financial support provided by Universitas Jenderal Soedirman, which was provided in accordance with the Fundamental Research Program managed by the Institute for Research and Community Service (LPPM). In addition, authors would like to thank the Hydraulic and Environmental Laboratory of the Engineering Faculty, Universitas Jenderal Soedirman, for the testing facility, and P.T. Reasuransi MAIPARK Indonesia for research collaboration.

## Conflicts of Interest

The authors declare no conflict of interest. The funders had no role in the design of the study; in the collection, analyses, or interpretation of data; in the writing of the manuscript; or in the decision to publish the results.

## AI Use Statement

The authors used ChatGPT-5 solely for grammar checking, sentence structure refinement, and improving the readability of the English text in this manuscript. The authors take full responsibility for all academic content, including all ideas, data, analyses, and conclusions presented herein. The use of AI was thoroughly reviewed and supervised by the authors.

## Appendix A

**Table A1.** Descriptions of nodes.

| Route | Node | Description | Route | Node | Description |
|---|---|---|---|---|---|
| R-1 | A | Citepus Beach | R-2 | A | Palabuhanratu Beach |
| | B | Gas station of Citepus | | B | Bend in the road |
| | C | Batu Alam Bungalows & Apartment | | C | Parluhutan lodge |
| | D | Building material store Berkah Citepus | | D | Intersection |
| | E | Three-way junction Citepus Cibudus | | E | Three-way junction |
| | J | Small alley | | G | Homestay Syakila |
| | F | Warkop & Sembako 41 | | F | Intersection |
| | G | MI Citepus Hilir | | L | SMP/SMA IT Al Fardiyatussaadah |
| | H | Volleyball court Leotek | | H | Three-way junction |
| | I | Islamic boarding school Miftahul Falah | | I | Bintan travel |
| | | | | J | Three-way junction |
| | | | | K | Citepus Girang complex |
| | | | | M | Yasfa orphanage Foundation |
| R-3 | A | RM bu engkar | R-4 | A | Bunga Ayu Seaside Resort |
| | B | Three-way junction | | B | Three-way junction Wisma Bukit Indah |
| | C | Three-way junction | | C | Three-way junction Toko Baim |
| | D | Bend in the road | | D | Intersection RM Minang Jaya |
| | E | Intersection | | E | Three-way junction Gn. Butak SDIT Insan Cendikia |
| | F | Warung mang sanim | | F | Three-way junction Jl. Babadan |
| | G | Three-way junction | | G | Promotion building and development center |
| | H | Intersection | | H | School of SMKN 1 Palabuhanratu |
| | L | SMP IT Al Fardiyatussaadah / MTS Yasfa | | I | |
| | M | Yasfa Orphanage Foundation | | | |
| | I | Bintan travel | | | |
| | J | Three-way junction | | | |

**Table A1.** *Cont.*

| Route | Node | Description | Route | Node | Description |
|---|---|---|---|---|---|
| R-5 | A | Gadobangkong square | R-6 | A | Palabuhanratu market |
| | B | Three-way junction Jl. Kidang Kencana | | B | Bookstore cahaya fajar |
| | C | Three-way junction Jl. Sirnagalih | | C | Dealer of Honda |
| | D | Intersection | | D | Inna rented house |
| | E | Intersection | | E | Palabuhanratu square |
| | F | Intersection | | F | Office of Kesbangpol |
| | G | Gening bouquet | | G | Three-way junction |
| | H | Intersection | | H | Intersection empang raya street |
| | I | Tiara Astrie Salon | | I | Intersection pemda street |
| | J | School of SMPN 3 Palabuhanratu | | J | Intersection bebeng seafood |
| | K | Three-way junction | | K | School of SDN 03 Palabuhanratu |
| | L | Promotion building and development center | | L | Intersection CFC Palabuhanratu |
| | | | | M | Three-way junction |
| | | | | N | Three-way junction |
| | | | | O | Intersection jl. Dewi Sartika |
| | | | | P | Intersection jl. Dewi Sartika |
| | | | | Q | Al Ikhlas mosque |
| | | | | S | Internet kiosk |
| | | | | R | Three-way junction |
| | | | | T | Scool of SMK Al Fajar Palabuhanratu |
| R-7 | A | Wharf 2 Palabuhanratu | R-8 | A | Palabuhanratu Beach |
| | B | Small bridge | | B | Three-way junction |
| | C | Intersection | | C | Salted fish processing |
| | D | Three-way junction Canteen Umi | | D | Andira beach |
| | E | Three-way junction jl. majelis | | E | Jl. RinQueen bee |
| | F | Intersection Al Ikhlas mosque | | F | Damar Group House |
| | G | Intersection jalan majelis | | G | Intersection (Lapang Neglasari) |
| | H | Three-way junction | | H | Honje sand |
| | I | School of SMK Al Fajar Palabuhanratu | | | |
| R-9 | A | Kawasan biro perikanan | R-10 | A | Beach twenty Cipatuguran |
| | B | Three-way junction | | B | Three-way junction |
| | C | LPK Mutiara Sagara | | C | Bend in the road |
| | D | Three-way junction | | D | Three-way junction |
| | E | Jl. Pelita | | E | Three-way junction Almira Shop |
| | F | Jl. RinQueen bee | | F | Krisna Jaya Motor Service |
| | G | Damar Group House | | G | Intersection |
| | H | Intersection (Neglasari square) | | H | Intersection Alkhalifi Laundry |
| | I | Pasir Honje | | I | Bend in the road |
| | J | IPB Pelabuhan Diklat water | | J | Bend in the road |
| | K | Settlement (near Bukit Ibrahim) | | K | Three-way junction bakso restaurant |
| | | | | L | Three-way junction |
| | | | | M | School of PAUD TP melati |
| | | | | N | Three-way junction |
| | | | | O | Three-way junction |
| | | | | P | Three-way junction |
| | | | | Q | Intersection |
| | | | | R | Three-way junction Wuarlela Fam |
| | | | | S | Three-way junction |
| | | | | T | Three-way junction Zia Cell |
| | | | | U | Nuansa Photo Studio |
| | | | | V | Intersection Astrina Clinic |
| | | | | W | Intersection rented house Bayu |
| | | | | X | Intersection Aliansi Iphone Store |
| | | | | Y | Three-way junction |
| | | | | Z | Three-way junction |
| | | | | AA | Rehabilitation social home |

**Table A1.** *Cont.*

| Route | Node | Description | Route | Node | Description |
|---|---|---|---|---|---|
| R-11 | A | Mahira ro water | R-12 | A | Gate of Power House PLTU Palabuhanratu |
| | B | Three-way junction | | B | Three-way junction Jl. Pelita Cipatuguran |
| | C | Intersection | | C | Mini Stokist Melia Sehat Sejahtera |
| | D | Three-way junction Wuarlela Fam | | D | Three-way junction |
| | E | Three-way junction Zia Cell | | E | Three-way junction Andira Beach |
| | F | Three-way junction | | F | Intersection |
| | G | Three-way junction Mosque Jami Albahri | | G | Intersection |
| | H | Intersection Astrina Clinic | | H | Three-way junction |
| | I | Three-way junction | | I | Three-way junction Alfamart Cipatuguran |
| | J | Intersection rented house Bayu | | J | Panti Sosial Rehabilitasi + SDN Cipatuguran |
| | K | Nuansa photo studio | | K | Beach |
| | L | Intersection Aliasni Phone Store | | L | Three-way junction |
| | M | Three-way junction | | M | Three-way junction |
| | N | Three-way junction Alfa | | N | Three-way junction |
| | | | | O | Beach kampung perahu |
| | | | | P | Three-way junction dapur geulis jaya |
| | | | | Q | Three-way junction |

**Table A2.** Distance between node of evacuation routes.

| Route | Node | Distance (m) | Route | Node | Distance (m) | Route | Node | Distance (m) |
|---|---|---|---|---|---|---|---|---|
| R-1 | A–B | 82.09 | R-2 | A–B | 113.90 | R-3 | A–B | 114.44 |
| | B–C | 281.90 | | B–C | 30.00 | | B–C | 33.27 |
| | C–D | 100.48 | | C–D | 89.42 | | B–D | 32.67 |
| | D–E | 40.56 | | D–E | 131.37 | | C–E | 38.41 |
| | D–J | 84.18 | | D–G | 85.64 | | D–E | 35.17 |
| | E–F | 73.43 | | G–F | 102.26 | | E–F | 70.74 |
| | J–F | 71.26 | | E–F | 42.30 | | F–G | 25.23 |
| | F–G | 151.67 | | F–L | 69.75 | | G–H | 42.30 |
| | G–H | 71.89 | | F–I | 104.20 | | H–L | 69.75 |
| | H–I | 80.74 | | G–H | 152.40 | | H–I | 104.20 |
| | | | | H–J | 57.65 | | I–J | 23.67 |
| | | | | I–J | 23.67 | | J–K | 185.13 |
| | | | | J–K | 185.13 | | K–M | 119.10 |
| | | | | K–M | 119.10 | | | |
| R-4 | A–B | 43.70 | R-5 | A–B | 111.71 | R-6 | A–B | 118.90 |
| | B–C | 60.24 | | B–C | 198.73 | | B–C | 388.10 |
| | C–D | 161.21 | | C–D | 20.57 | | C–D | 55.29 |
| | C–E | 79.86 | | C–E | 96.47 | | C–E | 197.82 |
| | E–D | 104.00 | | D–F | 141.60 | | D–G | 183.57 |
| | D–F | 420.14 | | E–G | 128.42 | | E–F | 79.30 |
| | F–G | 114.41 | | F–G | 117.67 | | G–F | 13.22 |
| | G–H | 55.00 | | G–H | 175.28 | | F–I | 70.97 |
| | G–I | 147.20 | | H–I | 168.84 | | I–J | 139.52 |
| | | | | I–J | 158.74 | | H–K | 60.21 |
| | | | | J–K | 83.29 | | J–K | 45.88 |
| | | | | K–L | 122.44 | | E–L | 66.40 |
| | | | | | | | L–I | 78.80 |
| | | | | | | | C–M | 34.30 |
| | | | | | | | M–N | 145.63 |
| | | | | | | | M–O | 72.86 |
| | | | | | | | O–P | 29.84 |
| | | | | | | | P–Q | 90.62 |
| | | | | | | | N–S | 178.06 |
| | | | | | | | Q–R | 40.00 |
| | | | | | | | S–R | 65.41 |
| | | | | | | | R–T | 114.4 |
| | | | | | | | N–L | 85.82 |
| | | | | | | | L–U | 179.41 |
| | | | | | | | U–V | 44.10 |

**Table A2.** *Cont.*

| Route | Node | Distance (m) | Route | Node | Distance (m) | Route | Node | Distance (m) |
|---|---|---|---|---|---|---|---|---|
| R-7 | A–B | 36.72 | R-8 | A–B | 87.60 | R-9 | A–B | 33.23 |
| | B–C | 111.21 | | B–C | 113.20 | | B–C | 27.69 |
| | B–D | 104.49 | | C–D | 186.29 | | B–D | 91.71 |
| | D–E | 196.54 | | D–E | 371.00 | | C–D | 72.16 |
| | C–E | 151.2 | | E–F | 209.00 | | D–E | 55.81 |
| | E–F | 50.89 | | F–G | 87.12 | | E–F | 250.20 |
| | F–G | 31.52 | | G–H | 268.43 | | F–G | 209.00 |
| | G–H | 13.11 | | | | | G–H | 87.12 |
| | H–I | 300.00 | | | | | H–I | 268.43 |
| | I–J | 102.22 | | | | | I–J | 275.23 |
| | | | | | | | J–K | 309.45 |
| R-10 | A–B | 93.94 | R-11 | A–C | 30.51 | R-12 | A–B | 418.89 |
| | B–C | 25.43 | | A–B | 73.82 | | A–C | 118.04 |
| | C–E | 80.81 | | C–D | 73.22 | | C–D | 102.20 |
| | B–D | 73.14 | | B–D | 30.70 | | D–E | 242.42 |
| | D–E | 30.58 | | D–F | 39.15 | | E–F | 116.24 |
| | E–F | 66.70 | | C–E | 42.6 | | F–G | 66.14 |
| | A–G | 101.36 | | E–K | 113.01 | | B–H | 185.58 |
| | G–H | 30.37 | | F–H | 46.64 | | G–H | 184.15 |
| | H–I | 19.18 | | B–G | 41.97 | | H–J | 188.22 |
| | H–J | 45.28 | | B–F | 70.70 | | E–I | 148.27 |
| | J–K | 20.44 | | G–H | 63.20 | | I–J | 286.36 |
| | I–K | 46.91 | | G–I | 31.35 | | K–L | 116.05 |
| | K–M | 30.00 | | H–J | 31.48 | | K–M | 68.58 |
| | G–L | 77.45 | | I–J | 64.91 | | L–N | 43.29 |
| | L–M | 52.84 | | H–L | 78.54 | | M–O | 148.14 |
| | L–N | 57.41 | | J–M | 79.38 | | N–O | 129.74 |
| | M–O | 47.33 | | K–L | 151.66 | | O–P | 99.00 |
| | N–P | 10.66 | | L–M | 29.47 | | P–Q | 178.39 |
| | P–O | 30.53 | | M–N | 93.32 | | L–D | 132.05 |
| | P–Q | 100.04 | | N–O | 285.12 | | E–Q | 43.69 |
| | O–T | 113.86 | | E–F | 73.83 | | Q–I | 104.58 |
| | F–U | 260.46 | | Y–AA | 63.87 | | | |
| | Q–T | 43.20 | | Y–S | 96.02 | | | |
| | Q–R | 73.22 | | Y–Z | 80.41 | | | |
| | R–S | 39.15 | | AA–AB | 176.65 | | | |
| | Q–T | 42.60 | | Z–W | 28.69 | | | |
| | T–U | 113.01 | | S–T | 33.08 | | | |
| | S–V | 46.64 | | W–X | 28.36 | | | |
| | T–S | 73.83 | | T–U | 41.15 | | | |
| | X–Y | 29.47 | | W–U | 60.00 | | | |
| | V–W | 31.48 | | X–V | 60.62 | | | |
| | V–X | 78.54 | | T–P | 45.47 | | | |
| | W–Y | 79.38 | | U–Q | 44.79 | | | |
| | U–X | 151.66 | | V–R | 50.42 | | | |
| | Y–Z | 93.32 | | U–V | 29.17 | | | |
| | Z–AA | 285.12 | | P–L | 36.21 | | | |
| | | | | P–Q | 41.54 | | | |
| | | | | Q–R | 24.53 | | | |
| | | | | R–J | 35.07 | | | |
| | | | | L–J | 64.91 | | | |
| | | | | J–M | 79.38 | | | |
| | | | | M–N | 93.32 | | | |
| | | | | AB–N | 104.97 | | | |
| | | | | N–O | 285.12 | | | |

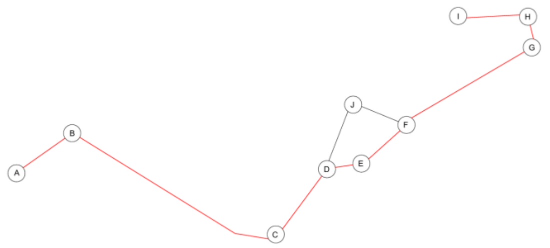


(**a**) Shortest route R-1.

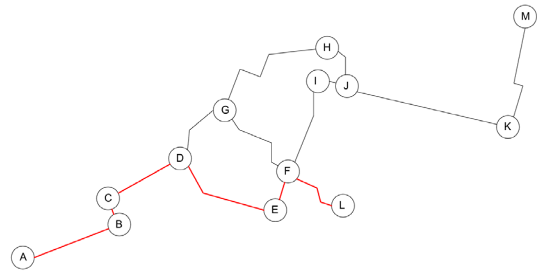


(**b**) Shortest route R-2 alternative 1.

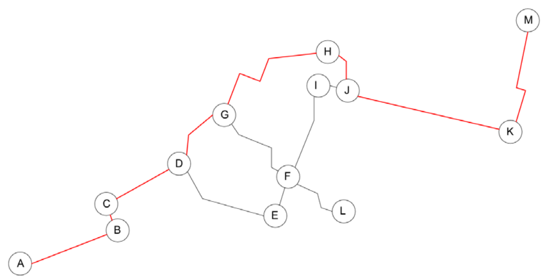


(**c**) Shortest route R-2 alternative 2.

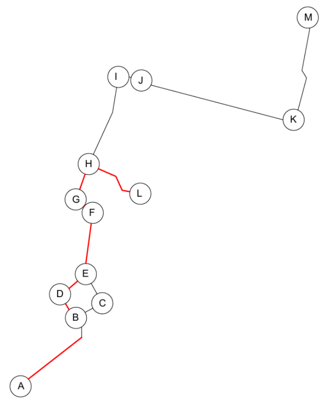


(**d**) Shortest route R-3 alternative 1.

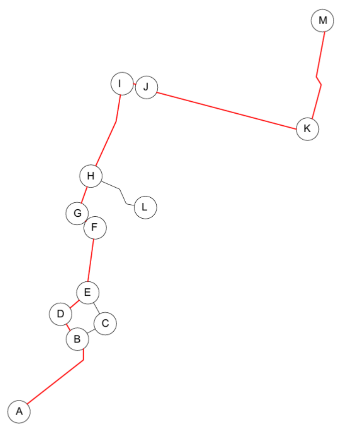


(**e**) Shortest route R-3 alternative 2.

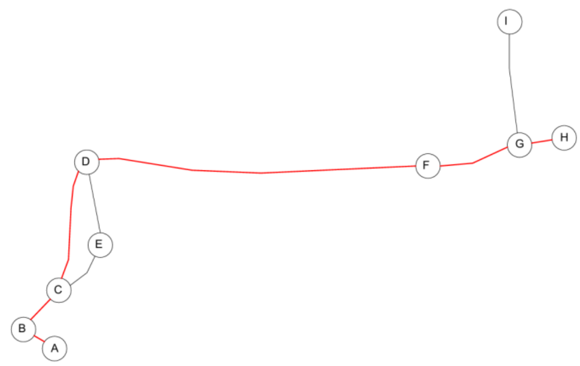


(**f**) Shortest route R-4 alternative 1.

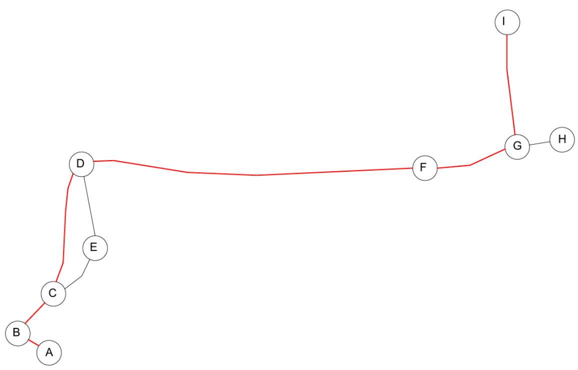


(**g**) Shortest route R-4 alternative 2.

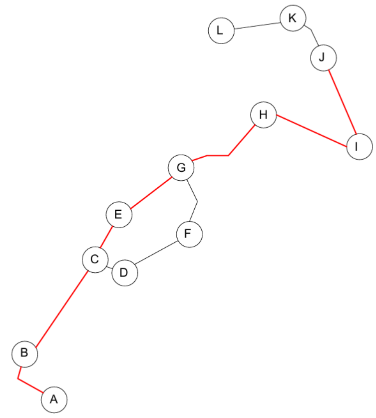


(**h**) Shortest route R-5.

**Figure A1.** *Cont.*

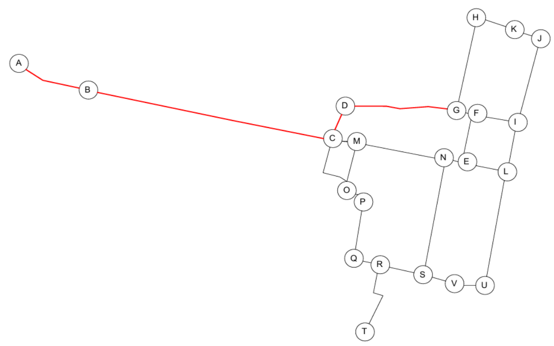


(**i**) Shortest route R-6 alternative 1.

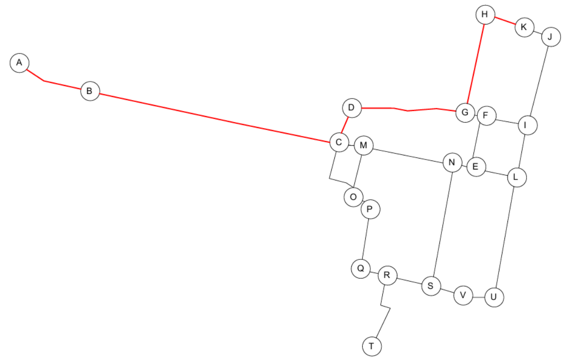


(**j**) Shortest route R-6 alternative 2.

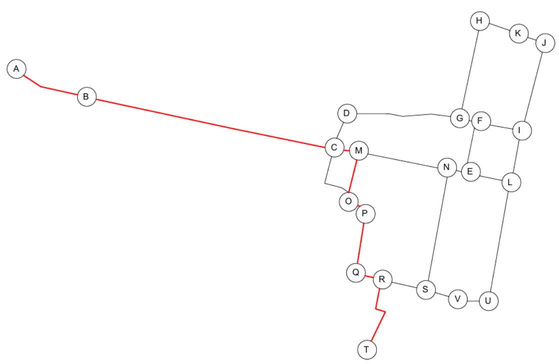


(**k**) Shortest route R-6 alternative 3.

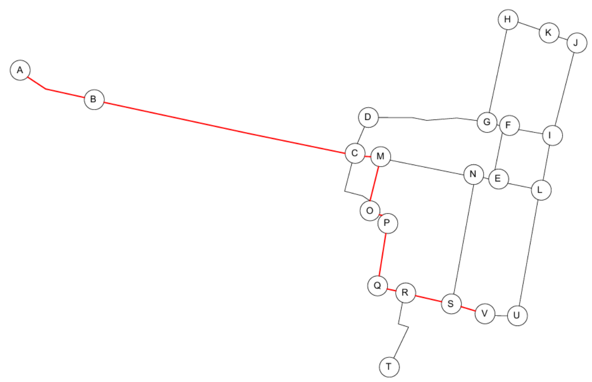


(**l**) Shortest route R-6 alternative 4.

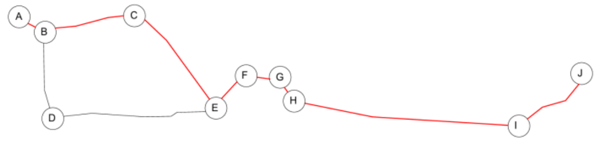


(**m**) Shortest route R-7.

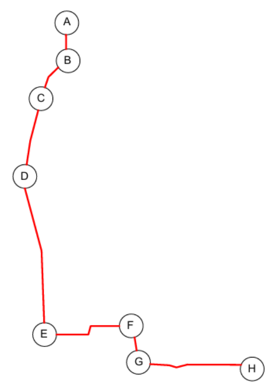


(**n**) Shortest route R-8.

**Figure A1.** *Cont.*

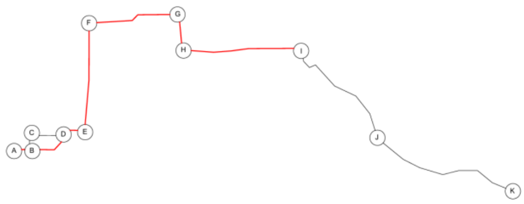


(**o**) Shortest route R-9.

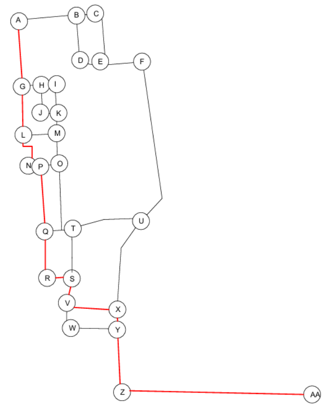


(**p**) Shortest route R-10.

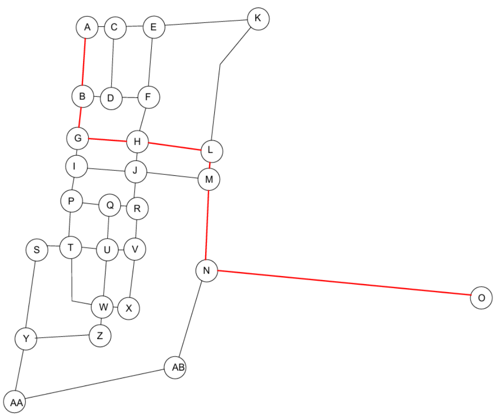


(**q**) Shortest route R-11 alternative 1.

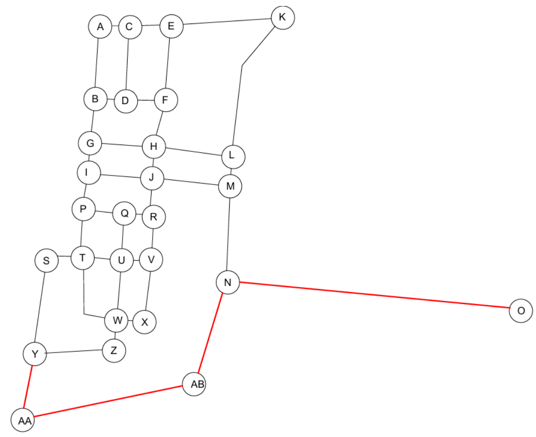


(**r**) Shortest route R-11 alternative 2.

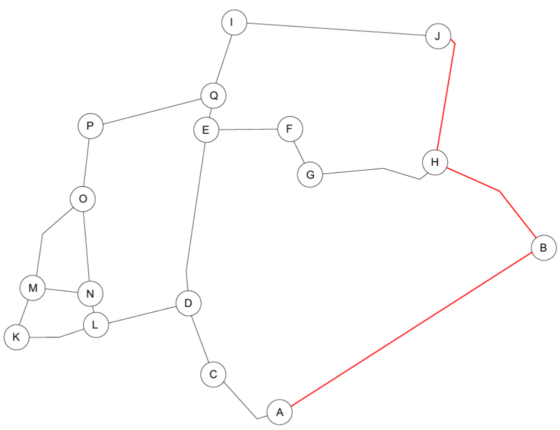


(**s**) Shortest route R-12 alternative 1.

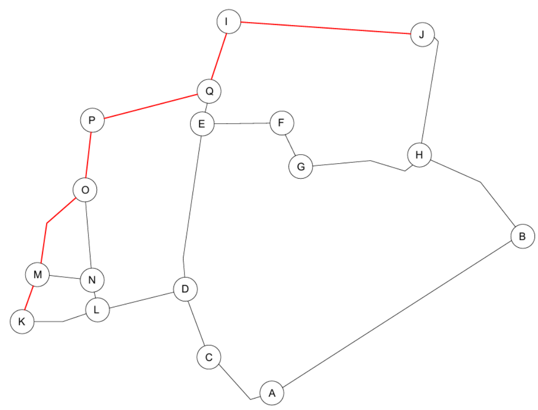


(**t**) Shortest route R-12 alternative 2.

**Figure A1.** Alternatives of evacuation routes.

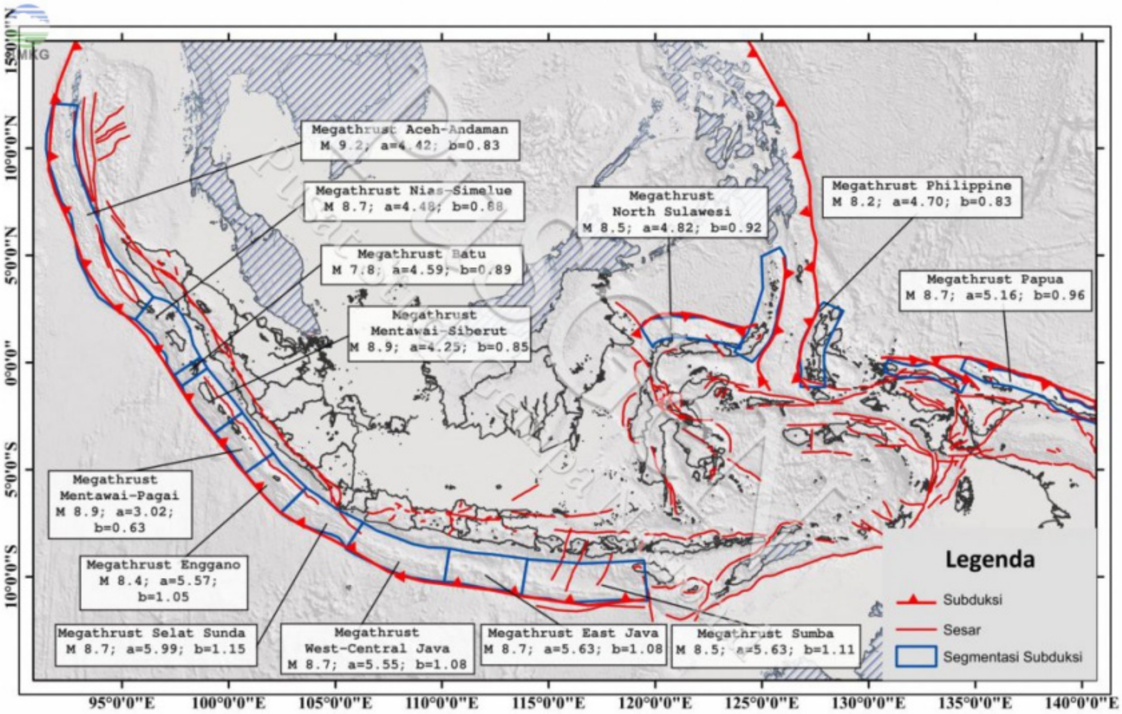


**Figure A2.** Earthquake sources in Indonesia.

Note: This study focuses on the green box where the Sunda Strait megathrust segment accounts for tsunami hazards in the study area (Palabuhanratu). The horizontal and vertical axis units are the same as indicated by the tick marks and label numbers, where for the horizontal axis, the distance between tick marks is 5° of longitude, and for the vertical axis, it is 5° of latitude, where 1° of longitude or latitude at the equator is equivalent to approximately 111.32 km.
Source: Map of Indonesian Earthquake Hazard Sources 2017.

# References


[1] Widiyantoro, S., Gunawan, E., Muhari, A., et al., 2020. Implications for megathrust earthquakes and tsunamis from seismic gaps south of Java Indonesia. Scientific Reports. 10, 15274.

[2] National Center for Earthquake Studies (PuSGeN), 2025. Indonesia's Earthquake Source and Hazard Map for 2024. Ministry of Public Work: Jakarta, Indonesia. (in Indonesian)

[3] Aziza, B., Muntasib, E.K.S.H., Hermawan, R., 2023. Impact of Tourism Activity in Ciletuh-Palabuhanratu Geopark (CPG), Sukabumi, West Java. Media Konservasi. 28, 43–50.

[4] Supendi, P., Widiyantoro, S., Rawlinson, N., et al., 2023. On the potential for megathrust earthquakes and tsunamis off the southern coast of West Java and southeast Sumatra, Indonesia. Natural Hazards. 116, 1315–1328.

[5] Gulo, E.R., Koestoer, R.H.S., 2024. Comparison of coastal tourism destination management against natural disasters of New Zealand and Indonesia. ASEAN Natural Disaster Mitigation and Education Journal. 1(2). DOI: https://doi.org/10.61511/andmej.v1i2.2024.377

[6] National Disaster Management Agency (BNPB), 2025. National Disaster Management Agency Regulation Number 1 of 2025 concerning the National Disaster Management Plan for 2025–2029. BNPB: East Jakarta, Indonesia. (in Indonesian)

[7] Lavrentiev, M., Lysakov, K., Marchuk, A., et al., 2021. Algorithmic Design of an FPGA-Based Calculator for Fast Evaluation of Tsunami Wave Danger. Algorithms. 14(12), 343.

[8] Wang, X., 2009. User Manual for COMCOT Version 1.7 (First Draft). GNS Science (Institute of Geological & Nuclear Sciences): Lower Hutt, New Zealand.

[9] Mohamed, E.S., Regina, M.Y., 2025. Implementation and validation of the TIMPULSE-SIM model for predicting tsunami wave behavior in the 2024 Kyushu, Hyuganada sea and 2011 Tohoku, Honshu tsunamis in Japan region. Natural Hazards. 121, 6921–6953.

[10] Le Quéré, P.A., Nistor, I., Mohammadian, A., 2020. Numerical Modeling of Tsunami-Induced Scouring around a Square Column: Performance Assessment of FLOW-3D and Delft3D. Journal of Coastal

Research. 36(6), 1278–1291.

[11] Borzì, L., Scala, P., Distefano, S., et al., 2024. Tsunami propagation and flooding maps: An application for the Island of Lampedusa, Sicily Channel, Italy. Earth Surface Processes and Landforms. 49, 4842–4861.

[12] Deltares System, 2012. Delft3D-FLOW User Manual: Simulation of Multi-Dimensional Hydrodynamic Flows and Transport Phenomena, Including Sediments. Deltares: Delft, The Netherlands

[13] Scala, A., Lorito, S., Escalante Sánchez, C., et al., 2024. Assessing the Optimal Tsunami Inundation Modeling Strategy for Large Earthquakes in Subduction Zones. Journal of Geophysical Research: Oceans. 129(9), e2024JC020941.

[14] Sedeño-Noda, A., Colebrook, M., 2019. A biobjective Dijkstra algorithm. European Journal of Operational Research. 276(1), 106–118.

[15] Zhu, Y., Li, H., Wang, Z., et al., 2022. Optimal Evacuation Route Planning of Urban Personnel at Different Risk Levels of Flood Disasters Based on the Improved 3D Dijkstra's Algorithm. Sustainability. 14(16), 10250.

[16] Mirahadi, F., McCabe, B.Y., 2021. EvacuSafe: A real-time model for building evacuation based on Dijkstra's algorithm. Journal of Building Engineering. 34, 101687.

[17] Li, B., Hou, J., Wang, X., et al., 2023. High-Resolution Flood Numerical Model and Dijkstra Algorithm Based Risk Avoidance Routes Planning. Water Resources Management. 37(8), 3243–3258.

[18] Bhat, R., Rao, P.K., Kamath, C.R., et al., 2024. Comparative analysis of Bellman-Ford and Dijkstra's algorithms for optimal evacuation route planning in multi-floor buildings. Cogent Engineering. 11(1), 2319394.

[19] Pierro, R., Ember, C.R., Pitek, E., et al., 2022. Local knowledge and practice in disaster relief: A worldwide cross-cultural comparison of coping mechanisms. International Journal of Disaster Risk Reduction. 76, 102988.

[20] Widiyanto, W., Santoso, P.B., Hsiao, S.-C., et al., 2019. Post-event field survey of 28 September 2018 Sulawesi earthquake and tsunami. Natural Hazards and Earth System Sciences. 19(12), 2781–2794.

[21] Widiyanto, W., Hsiao, S.-C., Chen, W.-B., et al., 2020. Run-up, inundation, and sediment characteristics of the 22 December 2018 Sunda Strait tsunami, Indonesia. Natural Hazards and Earth System Sciences. 20(4), 933–946.

[22] Shaw, R., Izumi, T., Djalante, R., et al. (Eds.), 2025. Two Decades from the Indian Ocean Tsunami: Key Challenges and Advancements. Springer Nature Singapore: Singapore.

[23] Isya, H.R.M., Arrasyid, R., Ihsan, H.M., et al., 2024. Tsunami Disaster Risk Reduction Strategy in Ciletuh–Palabuhanratu UNESCO Global Geopark. E3S Web Conference. 600, 01001.

[24] Environment and Road Safety Sector Directorate General of Highways, 2023. Tsunami Natural Disaster Evacuation Route Planning. Environment and Road Safety Sector Directorate General of Highways: Jakarta, Indonesia. (in Indonesian)

[25] Wells, D.L., Coppersmith, K.J., 1994. New empirical relationships among magnitude, rupture length, rupture width, rupture area, and surface displacement. Bulletin of the Seismological Society of America. 84(4), 974–1002.

[26] Blaser, L., Kruger, F., Ohrnberger, M., et al., 2010. Scaling Relations of Earthquake Source Parameter Estimates with Special Focus on Subduction Environment. Bulletin of the Seismological Society of America. 100(6), 2914–26.

[27] Shibayama, T., Esteban, M., Nistor, I., et al., 2013. Classification of Tsunami and Evacuation Areas. Natural Hazards. 67, 365–386.

[28] Fathianpour, A., Evans, B., Babaeian Jelodar, M., et al., 2024. Environmental factors in tsunami evacuation simulation: Topography, traffic jam, human behaviour. Natural Hazards. 120, 12797–12815.

[29] Chen, C., Mostafizi, A., Wang, H., et al., 2022. Evacuation behaviors in tsunami drills. Natural Hazards. 112(1), 845–871.

[30] Nakaya, N., Nemoto, H., Yi, C., et al., 2018. Effect of tsunami drill experience on evacuation behavior after the onset of the Great East Japan Earthquake. International Journal of Disaster Risk Reduction. 28, 206–213.

[31] Gowan, M.E., Sloan, J.A., Kirk, R.C., 2015. Prepared for what? addressing the disaster readiness gap beyond preparedness for survival. BMC Public Health. 15, 1139.

[32] Sofyan, H., Rahmatina, G., Hidayati, A., et al., 2025. Are we prepared for the next one? Evaluating community evacuation preparedness 20 years after the Indian Ocean tsunami. International Journal of Disaster Risk Reduction. 121, 105430.

[33] United Nations Office for Disaster Risk Reduction, 2015. Sendai Framework for Disaster Risk Reduction 2015–2030. UNDRR: Geneva, Switzerland.

[34] Ronkay, F., Molnar, B., Gere, D., et al., 2021. Plastic waste from marine environment: Demonstration of possible routes for recycling by different manufacturing technologies. Waste Management. 119, 101–110.
[35] Dong, L., Dong, C., Zhi, W., et al., 2024. A comprehensive approach to physical recycling of hazardous waste HDPE industrial drums: Overcoming challenges in safety and foam interference. Chemical Engineering Journal. 497, 154502.
[36] Amaratunga, D., Haigh, R., Dias, N. (Eds.), 2021. Multi Hazard Early Warning and Disaster Risks. Springer International Publishing: Cham, Switzerland.
[37] Nallapaneni, M.K., Hait, S., Priya, A., et al., 2023. From Trash to Treasure: Unlocking the Power of Resource Conservation, Recycling, and Waste Management Practices. Sustainability. 15(18), 13863.
[38] Rahmafitria, F., Sukmayadi, V., Suryadi, K., et al., 2021. Disaster management in Indonesian tourist destinations: how institutional roles and community resilience are mediated. Worldwide Hospitality and Tourism Themes. 13(3), 324–339.
[39] Setyonegoro, W., Gusman, A.R., Hanif, M., et al., 2024. Typical of Tsunami Hazard Potential from Earthquake and Landslide Sources in Palabuhanratu Bay, Indonesia. Pure and Applied Geophysics. 181, 1381–1412.
[40] Bernard, E.N., 2023. Tsunami Preparedness: Is Zero Casualties Possible? Pure and Applied Geophysics. 180, 1573–1586.